SIMB
Society for Industrial Microbiology
and Biotechnology

CrossMark

Changes in biooxidation mechanism and transient biofilm characteristics by As(V) during arsenopyrite colonization with *Acidithiobacillus thiooxidans*

Hugo Ramírez-Aldaba[1,7] · Jorge Vázquez-Arenas[2] · Fabiola S. Sosa-Rodríguez[3] · Donato Valdez-Pérez[4] · Estela Ruiz-Baca[1] · Gabriel Trejo-Córdoba[5] · Miguel A. Escobedo-Bretado[1] · Luis Lartundo-Rojas[6] · Patricia Ponce-Peña[1] · René H. Lara[1]

Abstract

Chemical and surface analyses are carried out using Raman spectroscopy, X-ray photoelectron spectroscopy (XPS), scanning electron microscopy (SEM–EDS), atomic force microscopy (AFM), confocal laser scanning microscopy (CLSM), glow discharge spectroscopy (GDS) and extracellular surface protein quantification to thoroughly investigate the effect of supplementary As(V) during biooxidation of arsenopyrite by *Acidithiobacillus thiooxidans*. It is revealed that arsenic can enhance bacterial reactions during bioleaching, which can strongly influence its mobility. Biofilms occur as compact-flattened microcolonies, being progressively covered by a significant amount of secondary compounds (S_n^{2-}, S^0, pyrite-like). Biooxidation mechanism is modified in the presence of supplementary As(V), as indicated by spectroscopic and microscopic studies. GDS confirms significant variations between abiotic control and biooxidized arsenopyrite in terms of surface reactivity and amount of secondary compounds with and without As(V) (i.e. 6 μm depth). CLSM and protein analyses indicate a rapid modification in biofilm from hydrophilic to hydrophobic character (i.e. 1–12 h), in spite of the decrease in extracellular surface proteins in the presence of supplementary As(V) (i.e. stressed biofilms).

Keywords Arsenopyrite biooxidation · Stressed biofilms · *Acidithiobacillus thiooxidans* · Glow discharge spectroscopy · Supplementary As(V)

Introduction

Arsenic (As) dissemination is a serious environmental problem due to its toxic character by direct or indirect exposure to soil, air, and water [13]. This toxic element is released to the environment from natural and anthropogenic processes

✉ René H. Lara
lcrh75@ujed.mx; lcrh75@hotmail.com

1 Facultad de Ciencias Químicas, Departamento de Ciencia de Materiales, Laboratorio de Electroquímica y Análisis de Superficies, Universidad Juárez del Estado de Durango (UJED), Av. Veterinaria S/N, Circuito Universitario, Col. Valle del Sur, 34120 Durango, DGO, Mexico

2 Centro Mexicano para la Producción más Limpia, Instituto Politécnico Nacional, Avenida Acueducto S/N, Col. La Laguna Ticomán, 07340 Mexico City, Mexico

3 Crecimiento Económico y Medio Ambiente, Departamento de Economía, Universidad Autónoma

Metropolitana-Azcapotzalco (UAM-A), Av. San Pablo 180, Azcapotzalco, 02200 Mexico City, Mexico

4 Instituto Politécnico Nacional (IPN), UPALM, Edif. Z-4 3er Piso, 07738 Mexico City, Mexico

5 Centro de Investigación y Desarrollo Tecnológico en Electroquímica (CIDETEQ), Parque Tecnológico Querétaro-Sanfandila, 76703 Pedro Escobedo, QRO, Mexico

6 Instituto Politécnico Nacional (IPN), CNMN, Av. Luis Enrique Erro S/N, Unidad Profesional Adolfo López Mateos, Zacatenco, 07738 Mexico City, Mexico

7 Facultad de Ciencias Forestales, UJED, Av. Río Papaloapan S/N, Col. Valle del Sur, 34120 Durango, DGO, Mexico

∂ Springer

(i.e. water-bedrock weathering reactions, coal and steel production, mining activities) [1]. It is known that its occurrence, fate and mobilization can be affected by microbially mediated biogeochemical reactions (i.e. biooxidation, bioleaching), which considerably increase As dissemination [2]. Arsenopyrite (FeAsS) is the most important source of As in lithosphere, typically undergoing a significant biooxidation (and bioleaching) in soil and mining waste by *Acidithiobacillus ferrooxidans* and *A. thiooxidans* [3, 4]. To this concern, the study of arsenopyrite bioleaching has been mostly focused on understanding interactions with *A. ferrooxidans*, since this iron- and sulfur-oxidizing microorganism (IOM/SOM) presents an enhanced capacity to efficiently use the Fe^{2+}/Fe^{3+} cycle, and to some extent, to oxidize sulfur compounds (i.e. S^-, S^{2-}, S^0) [5, 6]. In contrast, the analysis of sulfur-oxidizing microorganisms (SOM), such as *A. thiooxidans*, has been barely examined in spite of its great capacity to efficiently remove passive sulfur coating layers (i.e. S_n^{2-}, S^0) limiting the proficiency of *A. ferrooxidans* [5, 7, 8]. Thus, the study of the arsenopyrite biooxidation mechanism by single *A. thiooxidans* would certainly enable a better understanding of its contribution in mixed cultures [9, 10, 18].

To date, the interaction (i.e. biooxidation) arising between *A. thiooxidans* and arsenopyrite (i.e. at the interfacial level) remains poorly described, and particularly, when this interaction is affected by challenging environmental conditions (i.e. variations in pH, temperature, heavy metals). Our previous investigations have simulated this biooxidation process using electrochemical experiments, and performed a rapid evaluation of the transient biofilm characteristics without providing a detailed assessment of the effect of As on bacterial reactions [11, 12]. Particularly, additional evaluations concerning the role of As on biooxidation mechanism (*A. thiooxidans* and arsenopyrite), transient biofilm characteristics and chemical surface speciation are herein addressed, in order to understand biogeochemical cycles of As and the bacterial reactions affecting intrinsic arsenopyrite behavior. Likewise, bioleaching processes of arsenopyrite occur in the presence of important concentrations of As in the system, which are generated by the chemical and biological alteration of arsenopyrite (and As-rich mining waste) [3, 14, 31]. Additionally, leaching (and non-leaching) bacteria secrete extracellular polymeric substances (EPS), which are mainly composed of polysaccharides, proteins and lipids [15]. These substances possess a relevant role during cell attachment to sulfide minerals (SM), promoting biofilm stability [16, 17, 19], whence it is also a major concern to assess the biofilms characteristics in the presence of As(V) during arsenopyrite colonization with *A. thiooxidans*. In order to account for the effect of high As contains affecting the arsenopyrite and *A. thiooxidans* interactions, and the corresponding arsenopyrite structure–activity relationships, Raman, GDS,

XPS, SEM–EDS, AFM, CLSM and extracellular surface protein determinations are combined to describe the following aspects: (1) The effect of supplementary As(V) on the biooxidation pathways, (2) analysis of protein synthesis in biofilms under the effect of supplementary As(V), and (3) influence of challenging environmental conditions on transient biofilm properties. It is expected that these results contribute to gain a better understanding of bacterial reactions occurring during bioleaching of arsenopyrite in the presence of As in industrial and natural environments.

Materials and methods

Arsenopyrite samples

Massive arsenopyrite samples were obtained from auriferous mining area at Velardeña, Durango, Northwest of Mexico [21]. Purity of arsenopyrite samples, mineralogical identification, and the corresponding construction of massive arsenopyrite electrodes (MAE) were carried out as indicated in previous papers [11, 12]. Likewise, electrochemical oxidation of these MAE specimens allows a rapid and significant generation of secondary compounds (i.e. S_n^{2-} and S^0) (Electronic Supplementary Material, ESM, Fig. S1), which was induced as described in Refs. [11, 12] for use in abiotic and biotic experiments. Metabolic capacity of *A. thiooxidans* was then stimulated by presence of S_n^{2-} and S^0 compounds on the eMAE surfaces (i.e. energy source), allowing its colonization on the substrate [7, 15].

Biofilm formation and biooxidation assays

The strain used in this study was *A. thiooxidans* ATCC no. 19377, which was cultivated as indicated in Refs. [11, 12]. Thus, 10 mL of this culture was used as inoculum in biooxidation assays. Sterilized eMAE was placed in 50 mL ATCC-125 culture medium containing ~10^7 cells mL^{-1} at pH 2.0 (batch system) under sterile conditions. These experiments were conducted in the presence of supplementary As(V) (0.2 M NaH$_2$AsO$_4\cdot$H$_2$O, JT Baker) [22, 23] aerobically incubated around 30 °C. Abiotic control assays were also carried out to establish a fair comparison between chemical and biological oxidation. The above supplementary As(V) concentration was chosen to induce biofilm stress. Although it is known that As (III) is more toxic than As (V) to biota, it is well known that bacteria *A. thiooxidans* have a complex system to eliminate As (V) via dissimilatory reduction of these species to As (III), utilizing complex *Ars-R*, *Ars-A*, *Ars-B* and *Ars-C* genes [14, 24, 25]. Negligible effects of As(V) are expected for planktonic cells at the beginning of biooxidation experiments, assuming that *A. thiooxidans* attaches fast enough to arsenopyrite as occurs for *A. ferrooxidans* in

similar systems [26]. The stability of As(V) compounds (i.e. $H_2AsO_4^-$) has been established according to observations published by Lu and Zhu [27]. Resulting eMAE surfaces after biooxidation process in the presence of supplementary As(V) are herein referred as 'biooxidized eMAE surfaces with As(V)', whereas those after produced abiotic oxidation with supplementary As(V) are referred as 'abiotic control eMAE surfaces with As(V)'. Abiotic control and biooxidized eMAE surfaces with As(V) were collected at 1, 12, 24, 48, 72 and 120 h, dried with a direct flow of chromatographic grade N_2, and prepared under inert conditions for surface analyses. All control and biooxidation assays were carried out at least by duplicate. Chemical and surface analyses obtained during biooxidation of arsenopyrite without the effect of supplementary As(V) can be consulted in our previous papers [11, 12].

Surface analysis

Sample preparation to conduct chemical and surface analyses (SEM–EDS, AFM, Raman, CLSM and GDS) for all type of MAE specimens has been described in our previous papers [11, 12]. Additionally, XPS analyses were carried out for a more detailed characterization of secondary sulfur compounds (i.e. S_n^{2-} and S^0) in MAE surfaces involving chemical bonding and composition. These studies were performed using a K-Alpha Thermo Scientific spectrometer with a monochromatized Al Kα X-rays source (1486.6 eV), running at a power of 150 W. XPS narrow scans were collected at 60 eV pass energy. To detect and compensate the charge shift of the core level peaks, O1 s peak position at 531.0 eV was used as an internal standard. The base pressure in the analytical chamber was about 10^{-9} mbar. Spectra were collected at a normal take-off angle (90°) and the analysis area was 400×400 μm^2. All XPS spectra and obtained quantities correspond to an average of three measurements in different points of each sample. XPS S2p core level was then analyzed with Avantage v5.979 software from Thermo Scientific and fitted using a typical pseudo-Voight function. A Shirley type background subtraction was used during fitting procedure. The pristine MAE sample was prepared in an argon atmosphere, whereas the rest of samples were prepared at room conditions.

Protein extraction

Protein analysis was performed in order to assess changes in biofilms and to connect these results with surface analysis and the effect of As(V). EPS-associated protein fraction (i.e. extracellular surface protein) was extracted from biofilms after biooxidation assays in the presence of supplementary As(V), according to experimental details provided in previous papers [11, 12]. To achieve this, four sterilized eMAE surfaces (~ 1 cm^2 of area) were placed into 50 mL of ATCC-125 culture medium containing ~ 10^7 cells/mL and 0.2 M of $NaH_2AsO_4 \cdot H_2O$ (JT Baker) at pH 2.0 (batch system) for each evaluated time. Normalization of data was performed by relating the protein concentration per eMAE-surficial area (1 cm^2). The protein concentration was determined by the Bradford method [28] by comparing the measured absorption values (UV–Vis 50 Bio-spectrophotometer) with those of a calibration range of albumin as standard concentration (1–30 mg mL^{-1}). This protocol enables the extraction of the EPS-associated protein fraction (i.e. avoiding heating of the system to decrease cell lysis), thus, allowing a quantitative assessment of the extracted proteins [29].

Results and discussion

Figure 1 shows Raman spectra for abiotic control eMAE surfaces with As(V) after 120 h (Fig. 1a) and biooxidized eMAE surfaces with As(V) collected after 1, 12, 24, 48, 72 and 120 h of assay (Fig. 1b1–b6, respectively). In order to compare the biological oxidation in the presence and absence of supplementary As(V), all results for the studied system without the effect of As(V) (i.e. Raman, SEM, CLSM, proteins extraction) should be consulted in Ramirez-Aldaba et al. [11, 12]. Abiotic control eMAE surfaces with As(V) essentially show the same secondary compounds (i.e. pyrite-like phases, at 329 and 363 cm^{-1}, Fig. 1a), which is similar to that observed for abiotic control samples in the absence of As(V) [12]. This finding suggests minor or negligible precipitation of As-bearing secondary compounds during chemical weathering due to the absence of bacteria (i.e. contamination), including biooxidation experiments. Raman spectra for biooxidized eMAE surfaces with As(V) indicated the presence of well-defined S^0 at 1 h (134, 201, 455 cm^{-1}, Fig. 1b1), and S_n^{2-} at 12 h (473 cm^{-1}, Fig. 1b2, Table S1 in [12]). Additionally, a mixture of pyrite-like and S^0/S_n^{2-} phases was identified at 24 h (353, 393 cm^{-1}; 125, 204, 462 cm^{-1} spectrum i; 462 cm^{-1} spectrum ii, Fig. 1b3), and S_n^{2-} compounds after 48 h (467 cm^{-1}, Fig. 1b4). Finally, S^0 was identified at 72 h (125, 204, 461 cm^{-1}, Fig. 1b5) and a mixture of pyrite-like and S_n^{2-} after 120 h (355, 366; 473 cm^{-1}, Fig. 1b6, Table S1 in [12]). A general comparison between Raman spectra obtained for biooxidized eMAE surfaces [12] and biooxidized eMAE surfaces with As(V) (Fig. 1b1) revealed a delay in early stages of biooxidation process in the presence of supplementary As(V), since well-defined S^0 was observed in both systems, indicating minor *A. thiooxidans* and arsenopyrite interaction (i.e. 1 h). This inhibition in the biooxidation process represents sluggishness in the colonization mechanisms in which *A. thiooxidans* adjust to face this microenvironment (i.e. As) [18, 30, 31]. These findings also indicate that *A. thiooxidans* sustain biooxidation activity after incipient stage (i.e. stressed biofilms, 12 to
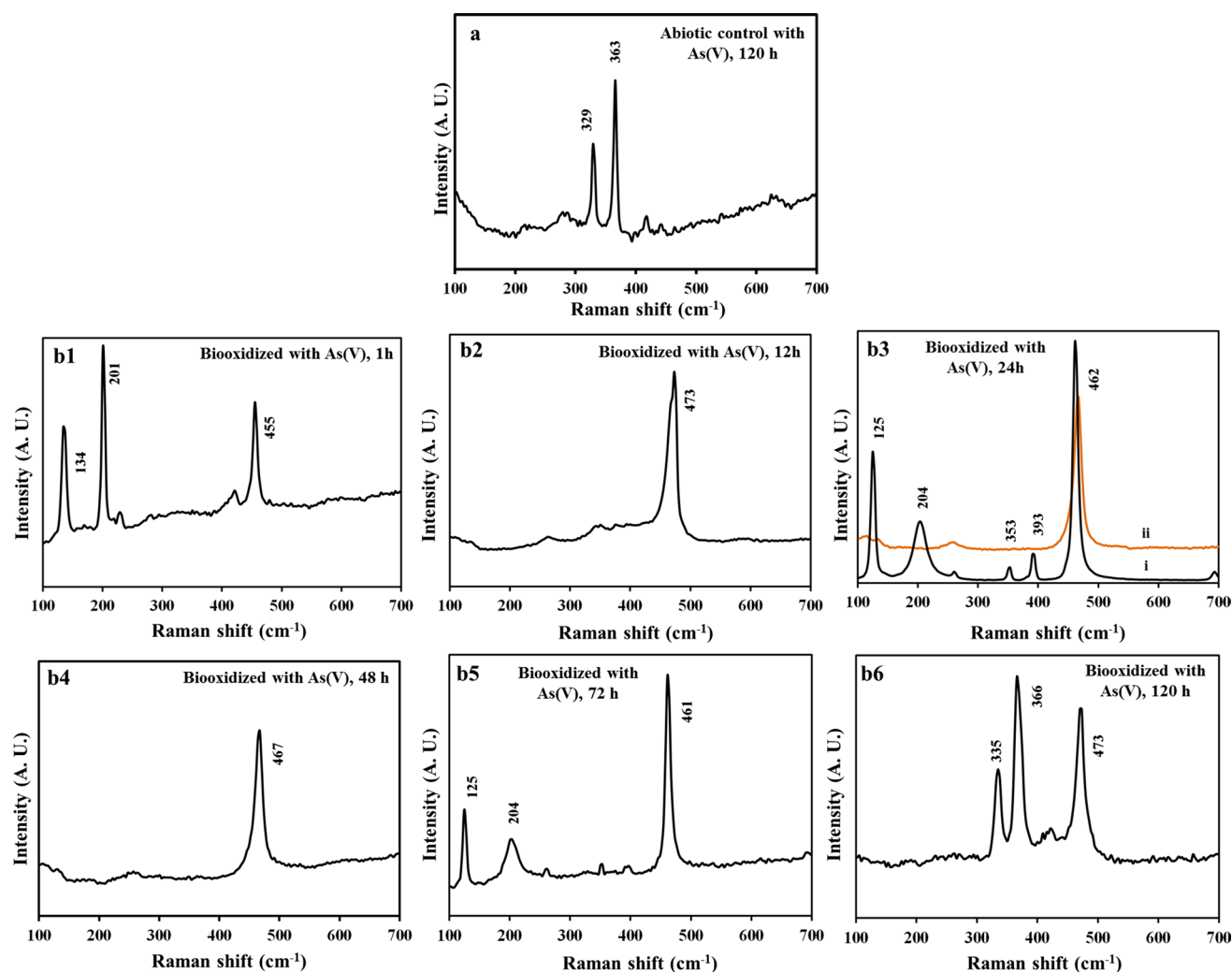
Fig. 1 Raman spectra obtained from abiotic control with As(V) at 120 h (**a**), and biooxidized eMAE samples with As(V) for 1 (**b1**), 12 (**b2**), 24 (**b3**, spectra i, ii), 48 (**b4**), 72 (**b5**) and 120 h (**b6**). Abiotic control eMAE surfaces contained similar secondary compounds for all analyzed times. 60 s of collection time. $\lambda = 514$ nm. 25 A

120 h), which involves a different biooxidation process (or mechanism) regarding previous observations (i.e. chemical surface speciation), and in agreement with literature [2, 23].

Figure 2 shows the corresponding fitting procedures of S2p spectra for typical pristine MAE surface (Fig. 2a), eMAE surface (without leaching) (Fig. 2b), and samples collected after 24 and 120 h in the presence (Fig. 2c″, d″, respectively) and absence (Fig. 2c′, d′, respectively) of supplementary As(V). Additionally, Figure S2 shows fitting procedures of S2p spectra for samples collected after 48 h in the presence and absence of supplementary As(V) and the corresponding control sample. A summary of S2p peak parameters and the corresponding binding energies to identify chemical bonding of sulfur species are listed in Tables S2 and S3, respectively. The S2p spectrum in the pristine MAE surface shows a major doublet, with a S2p$_{3/2}$ component located at ~ 162.3 eV, commonly assigned to

$(AsS)^{2-}$ species in mineral crystal lattices (Fig. 2a, Tables S2 and S3). A second minor doublet with a S2p$_{3/2}$ component at ~ 161.3 eV reflects the presence of S_2^{2-} species. Finally, a third doublet with a S2p$_{3/2}$ component arising at ~ 164.0 eV is attributed to S^0/S_n^{2-} species due to uncontrolled oxidation (Table S2, [32–34]). The S2p spectrum of the eMAE specimen reveals the additional presence of sulfate (i.e. ~ 168.5 eV) and sulfite (i.e. SO_x^{2-})-like species (~ 166.3 eV) (Fig. 2b, Tables S2 and S3). This spectrum also shows the concomitant decrease of $(AsS)^{2-}$ species (~ 162.3 eV) and the progressive enrichment of a mixture of S_n^{2-} and S^0 compounds (~ 163.3 eV) (Fig. 2b, Tables S2 and S3). These findings confirm the presence of S^0 and S_n^{2-} coating layers on the eMAE specimens, in agreement with Raman study (Table S2, [12]). The higher production of S_2^{2-} species (Fig. 2b) regarding the pristine MAE specimen (Fig. 2a) is presumably associated with the formation
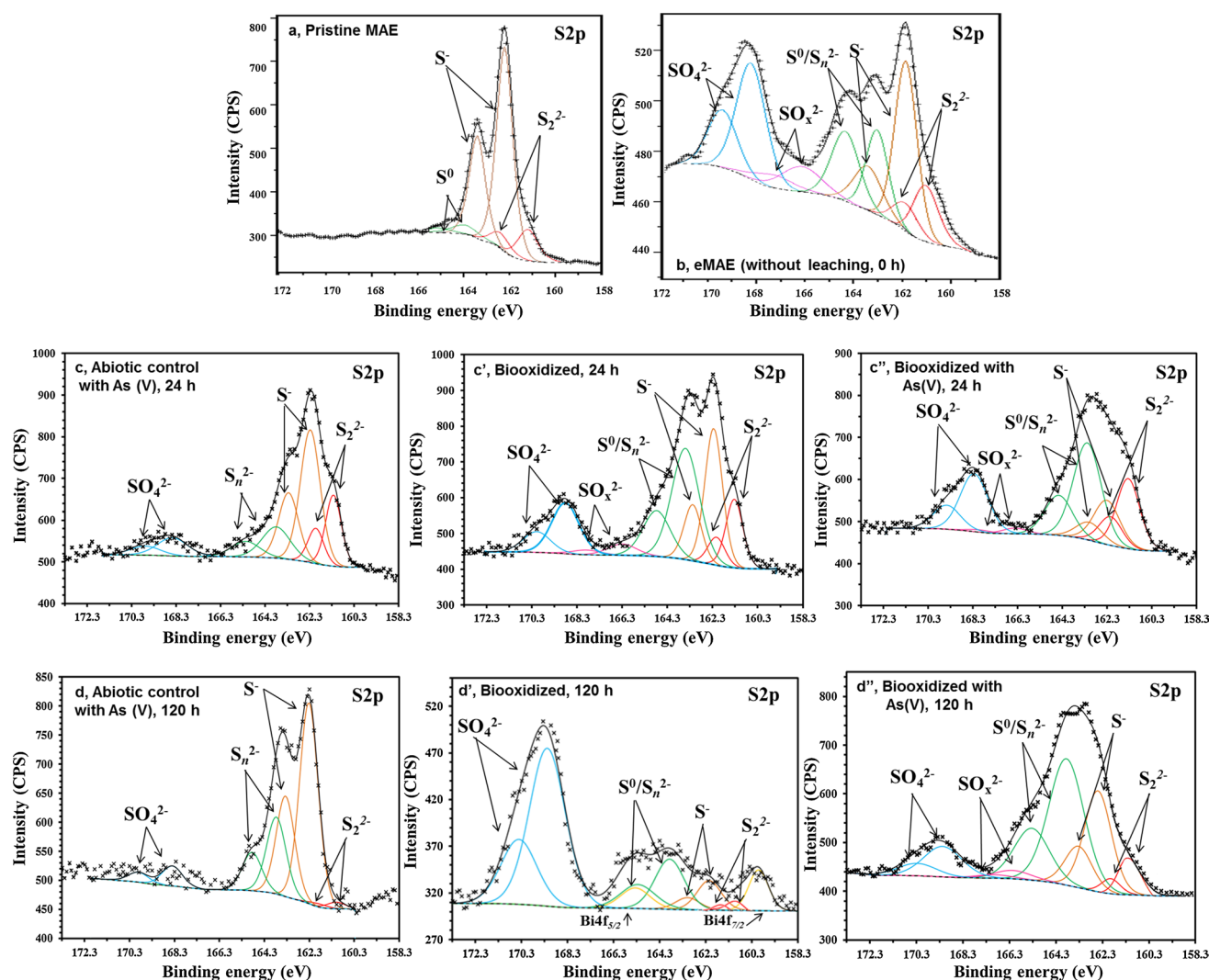
Fig. 2 XPS S2p spectra collected for pristine MAE (**a**), eMAE specimen (without leaching) (**b**), abiotic control surfaces (**c**, **d**), biooxidized eMAE surfaces (**c′**, **d′**) and biooxidized eMAE surfaces with As(V) (**c″**, **d″**) after 24 and 120 h of assay, respectively

of the pyrite-like compound (i.e. FeS_2, S_2^{2-}, i.e. [34]); also in connection with Raman study (Fig. 1).

The fitting of the S2p spectra for abiotic control eMAE samples in general excludes the presence of the sulfite (SO_x^{2-})-like species and shows minor formation of sulfates (Figs. 2c, d, S2, for 24, 48 and 120 h, respectively; Tables S2 and S3). These findings suggest a trend for the progressive accumulation of refractory secondary compounds (i.e. S^0, S_n^{2-}, pyrite-like); in agreement with Raman study (Fig. 1a). The fittings of the S2p spectra for biooxidized eMAE surfaces (i.e. without As(V)) (Figs. 2c′, d′, S2, for 24, 48 and 120 h, respectively) and biooxidized eMAE surfaces with As(V) (Figs. 2c″, d″, S2, for 24, 48 and 120 h, respectively) show clear differences regarding controls and between biooxidized eMAE surfaces without As(V). These spectra indicate variations in the composition and amount of secondary sulfur compounds. The presence of sulfates is the

highest one after 120 h of assay (Fig. 2d′, Tables S2 and S3) if compared against other biooxidation times. Additionally, higher production of S^0 and S_n^{2-} is clearly identified whence the presence of SO_x^{2-}-like species is negligible (Fig. 2c′, d′, S2, for 24, 48 and 120, respectively, Tables S2 and S3). These suggest that most important stage of biooxidation process occur after 120 h in the presence and absence of As(V), in spite of sluggishness observed in early biooxidation in the presence of As(V). The main differences identified in the S2p spectra of biooxidized eMAE surfaces with As(V) regarding biooxidized eMAE samples indicated enhanced cyclic variations for S_n^{2-}, S^0 and soluble sulfur species (Fig. 2, Tables S2 and S3), thus, revealing dynamic characteristics for transient bacteria and arsenopyrite interactions. Note that S2p spectrum after 120 h of assay requires an additional doublet, which is associated to Bi_xO_y-like phase involving the main signal of $Bi4f_{7/2}$ at ~159.9 eV (Fig. 2d′,

Tables S2 and S3). This element emerges from mineral bulk impurities in arsenopyrite specimens collected from skarn or vein ore deposits [32].

The understanding of incipient structure–activity relationships (i.e. concentration vs depth profiles) was previously determined at 12 h of biooxidation in the absence of supplementary As(V) [12]. In order to investigate more profoundly the intrinsic arsenopyrite biogeochemical behavior (i.e. S) during bacterial reactions in the presence of As(V) and for a more extended time interval, eMAE samples were analyzed using GDS (i.e. 6 μm depth) after 24 and 120 h in the presence and the absence of supplementary As(V). Figure S3 also exhibits GDS analysis for biooxidized sample with As(V) after 12 h of assay for a fair comparison. Figure 3 exhibits spectra for this technique of abiotic control eMAE (Fig. 2a, b), biooxidized eMAE surfaces (Fig. 2a′, b′) and biooxidized eMAE surfaces with As(V) (Fig. 2a″, b″) after 24 and 120 h of assay, respectively. GDS spectra for pristine MAE, eMAE and controls and biooxidized samples without As(V) can be consulted in Ramírez-Aldaba et al. [12]. GDS spectra of pristine MAE and eMAE surfaces display a typical behavior for a FeAsS structure and a remarkable production of sulfur compounds around 90% wt ([12], from 0 to ~4.5 μm in depth), respectively, confirming the starting surface condition for abiotic control and biooxidation assays, in agreement with XPS (Fig. 2b). The presence of Mn and Mo (1–6 μm depth) is a natural content in arsenopyrite lattices (i.e. impurities), since these elements were not previously observed in Fig. 1. Additionally, the

presence of carbon in eMAE surface (Fig. 3) and abiotic controls (Figs. 3a, b) were associated to readily adsorption of CO_2 on mineral surface [33]. Accordingly, the increment of carbon between 1 and 6 μm depth was then associated to the rise of surface area (i.e. increment or higher accumulation of secondary compounds) due to chemical oxidation of arsenopyrite [11]. The presence of higher amounts of carbon in concentration vs. depth profiles for all type of biooxidized eMAE surfaces was mainly associated to occurrence of EPS composing biofilms, in agreement with Zhu et al. [34]. Note that concentration of sulfur compounds was similar between eMAE surface [12] and biooxidized eMAE surface with As(V) after 1 h (data not shown), hence, confirming the observations made above by Raman and XPS studies (i.e. sluggish incipient biooxidation).

Concentration vs. depth profiles obtained for abiotic control eMAE surfaces indicated the progressive accumulation of secondary sulfur compounds, which is more evident after 120 h of abiotic oxidation (Fig. 3b). In contrast, a significant cyclic production-depletion process of sulfur compounds was identified for biooxidized eMAE samples after 12 (Fig. S3) and 24 h (Fig. 3a′) of assay, whereby sulfur compounds were virtually depleted after 120 h of biooxidation (Fig. 3b′). Remarkably, biooxidation process in the presence of supplementary As(V) indicated proficient bacterial capacity to sustain cyclic biooxidation, as indicated by testing after 24 and 120 h of assay (Figs. 3a″, b″, respectively). These findings and the intense changes in the concentration-depth profiles (i.e. sulfur compounds, 6 μm) identified for the rest of the
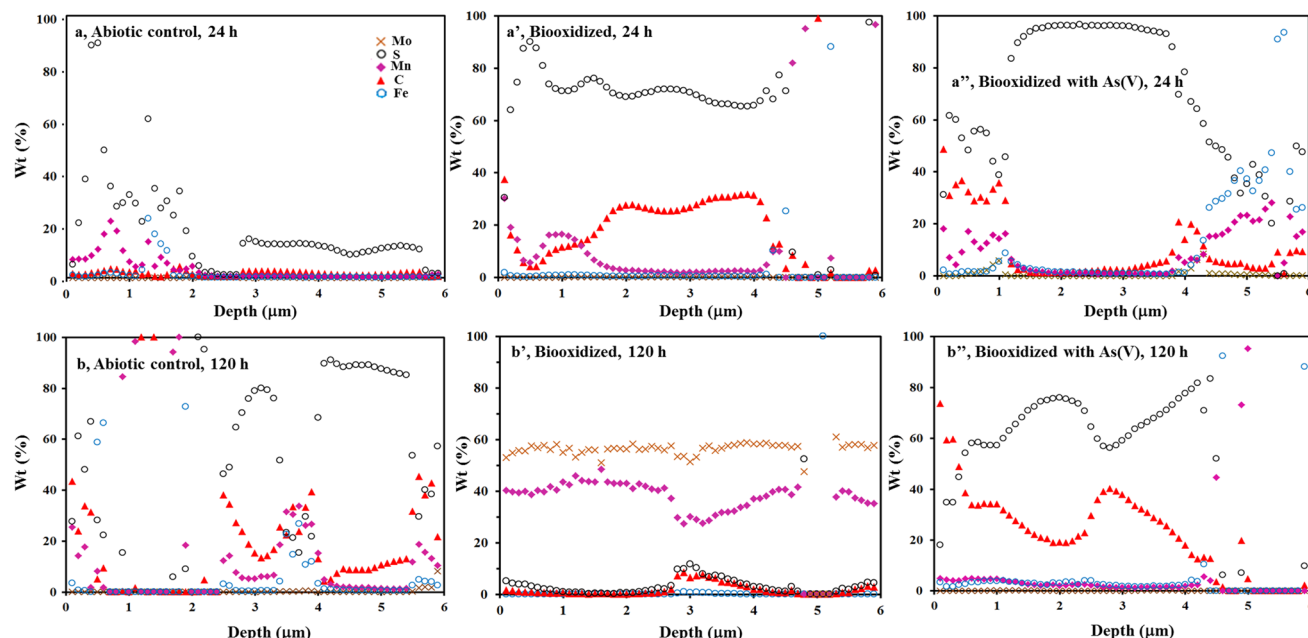

Fig. 3 Global Discharge Spectroscopy spectra for abiotic control eMAE surfaces (**a**, **b**), biooxidized eMAE surfaces (**a′**, **b′**) and biooxidized eMAE surfaces with As(V) (**a″**, **b″**) after 24 and 120 h of assay, respectively. Profiles for S, Fe, C, Mn and Mo are illustrated in the figure

biooxidized samples confirm that the bacterial mechanism has changed in the presence of supplementary As(V) (i.e. stressed biofilms). Some investigations have analyzed intrinsic arsenopyrite and pyrite biogeochemical behavior using quantitative X-ray photoelectron spectroscopy-based depth profiling (i.e. *A. ferrooxidans*) [34–36]. These reports indicated in general an enrichment of Fe, S and As compounds as a function of depth (i.e. 3.5 µm), which was directly associated with bacterial reactions mediating indirect *A. ferrooxidans* attachment. Figure 3 confirms a dynamic bacterial biooxidation behavior (i.e. cyclic production-depletion of secondary sulfur compounds, 1–6 µm depth) instead of a progressive accumulation of secondary compounds. However, this mechanism of biooxidation is sluggish in the initial stages, and even slower in the latest stages in the presence of supplementary As(V) (Fig. 3). These findings reveal a different bacterial interaction, which was associated with the type of *A. thiooxidans* attachment to arsenopyrite (i.e. direct) [11, 38], in comparison with typical *A. ferrooxidans* attachment (i.e. indirect) [6, 10, 37].

An assessment of the eMAE surface status was previously provided for 48 and 240 h of biooxidation in order to visualize biofilms evolution by AFM under the presence and absence of supplementary As(V) [11]. In the present study, this information is complemented with additional AFM observations in order to achieve a full and comprehensive description of surface processes under these conditions. Figure S4 shows typical images of abiotic control eMAE (Figs. S4a, S4b), and attached cells of *A. thiooxidans* on biooxidized eMAE (Figs. S4a′, S4b′) and biooxidized eMAE surfaces with As(V) (Figs. S4a″, S4b″) after 12 (i.e. incipient biofilms) and 72 h (i.e. well micro-colony structure development) of assay, respectively. The surface of the abiotic control eMAE samples shows bigger structures than those observed in the eMAE surface [11], after 12 and 72 h of chemical weathering (Fig. S4), respectively, which is consistent with progressive accumulation of refractory pyrite-like compounds (Fig. 1a). In the absence of supplementary As(V), biofilms undergo a transition from monolayer of attached cells with a typical size between 1 and 2 µm (Fig. S4a′, i.e. 12 h), in agreement with observations made by Liu et al. [38], to micro-colonies (Fig. S4b′, i.e. 72 h). Note that details associated with the underlying modified arsenopyrite surface and secondary compounds are distinguishable, thus, supporting direct cell attachment mediating arsenopyrite and *A. thiooxidans* interactions (Figs. S4a′, S4b′) [11]. Attached cells seem to be progressively embedded in the resulting secondary compounds (Fig. S4b′). A low cell density flattened-structure was distinguishable on the biooxidized eMAE surfaces with As(V) after 12 h (Fig. S4a″), while major formation of secondary compounds supports the idea that stressed biofilms induce dynamic biooxidation with the accelerated production of secondary compounds (i.e.

after 72 h, Fig. S4b″), in agreement with GDS observations (Fig. 3a″, b″). These findings provide a critical perspective on response of attached *A. thiooxidans* cells to altered arsenopyrite mainly in the presence of supplementary As(V), and offer an starting point for the understanding of SOM leaching cells behavior facing challenging environments (i.e. at the interfacial level).

Figure 4 shows SEM images complementary to previous assessments [11, 12] whereby the effect of supplementary As(V) on transient biofilm properties was further assessed. Therefore, Fig. 4 includes SEM–EDS analyses for abiotic control eMAE with As(V) after 120 h (for instance, Fig. 4a), and biooxidized eMAE samples with As(V) for all assayed times (Figs. 4b1–b5). The abiotic control samples in the presence of As(V) exhibited a similar topographic-morphologic behavior regarding abiotic control samples without supplementary As(V) [12], as well as the same secondary products in all sampled times (i.e. pyrite-like phase). This finding supports negligible precipitation of As-bearing compounds in abiotic control and all type of biooxidized surfaces induced by medium conditions (i.e. contamination), as previously discussed in the Raman study (Fig. 1a). The identification of secondary compounds was carried out by the energy-dispersive X-ray spectroscopy (data not shown). Figure 4 indicated the presence of spread attached cells in incipient stages (Fig. 4b1, b2), and also confirmed the occurrence of compact-flattened micro-colonies with high production of bacterial EPS in the presence of supplementary As(V) for later stages of biooxidation, as indicated by AFM (Fig. S4). These findings involving spread and few attached cells (Fig. 4b1, b2) enable to explain sluggishness in incipient biooxidation stages in the presence of supplementary As(V), in agreement with previous results (Figs. 1, 2, 3, S4) [39]. However, subsequent biooxidation stages indicated important formation of bacterial EPS composing compact-flattened micro-colonies in the presence of supplementary As(V) (Fig. 4b3–b5), thus, confirming occurrence of stressed biofilms interacting with secondary compounds (i.e. S_n^{2-}, S^0, pyrite-like) (Fig. 4b5). According to literature [19, 20, 40], the secretion of exopolysaccharides is a prerequisite of *A. ferrooxidans* cells for pyrite attachment, which could be a common requirement for all leaching bacteria when facing stressing conditions (i.e. As).

Figure 5 shows CLSM images for biooxidized eMAE samples with As(V) for all assayed times (Fig. 5a1–a6), complementary to AFM and SEM studies. In this figure, a merge between epifluorescence for exopolysaccharides (displayed originally in green) and lipids (display originally in red) was perceived. A compilation of epifluorescence data from cells forming biofilms in the presence of supplementary As(V) was depicted in Table S4. Likewise, CLSM images without the effect of supplementary As(V) can be consulted in [12], for comparison purposes. Figure 5
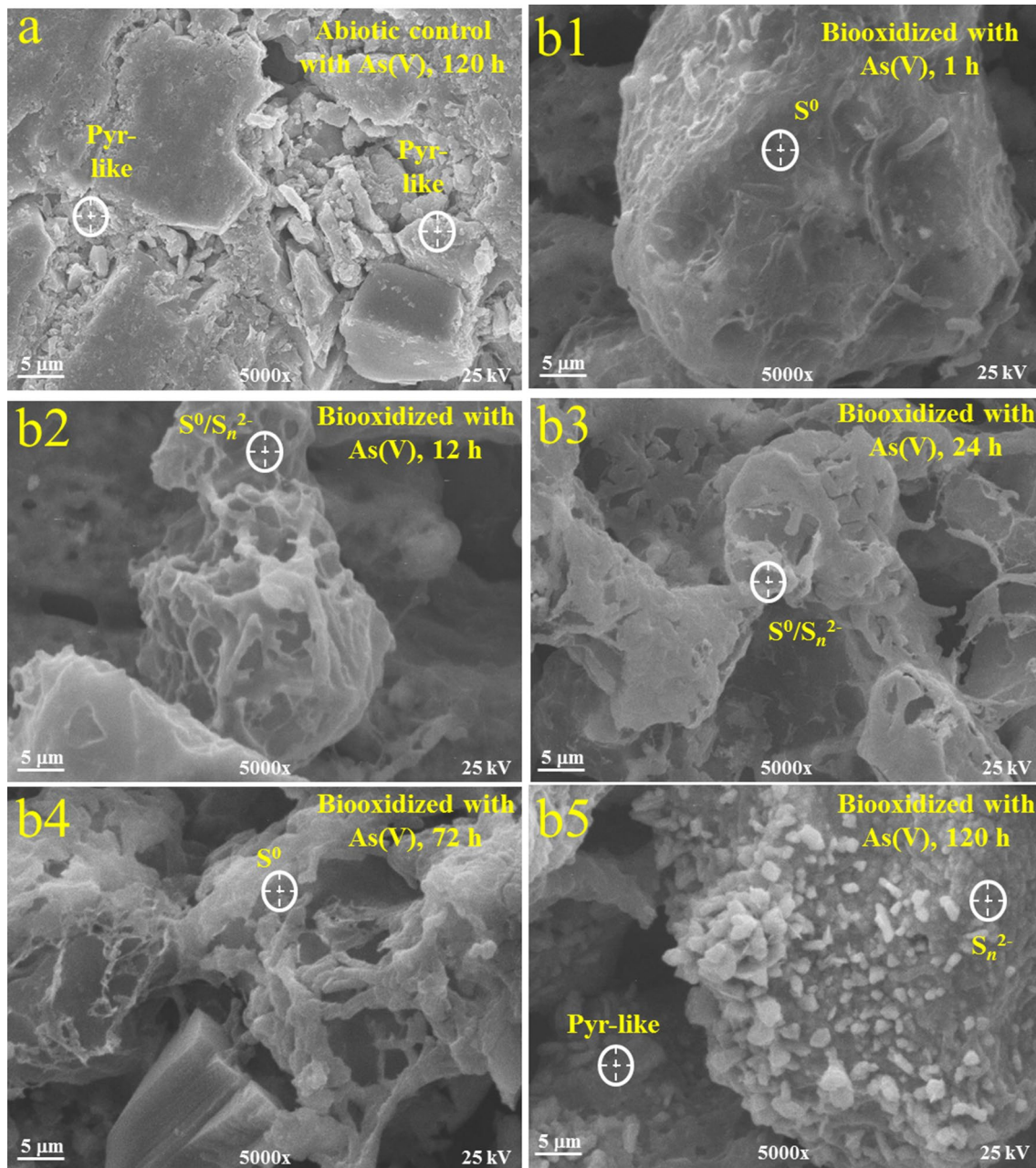
Fig. 4 Typical SEM images of the abiotic control eMAE surfaces with As(V) after 120 h of assay (**a**) and biooxidized eMAE surfaces with As(V) after 1 (**b1**), 12 (**b2**), 24 (**b3**), 48 (**b4**), 72 (**b4**), and 120 h (**b5**) of assay. Aspy = FeAsS; Pyr-like = pyrite-like; S_n^{2-} = polysulfide structures; S^0 = elementary sulfur (according to EDS analyses, $n = 10$)

confirmed the formation and evolution of stressed biofilms due to significant presence of extracellular lipids and exopolysaccharides (i.e. α-mannose, α-glucose) in bacterial EPS [39]; in agreement with previous observations of SEM–EDS study (Fig. 4). Additionally, sluggish incipient biooxidation was correlated with low cell density structure, higher production of exopolysaccharides and minor presence of extracellular lipids (i.e. 1 h, Fig. 5a1, Table S4). The cell density structure of biofilms increased between 24

and 72 h (Figs. 4b4, b5, 5a3, a5, respectively), thus, involving a noteworthy and rapid increment of extracellular lipids (i.e. yellow to red) to configure compact-flattened microcolonies since 12–24 h of biooxidation (Figs. 4b2–b3, 5a2–a3, respectively, Table S4). These findings indicated the establishment of a more hydrophobic surface (i.e. stressed biofilms and S_n^{2-}/S^0 compounds) due to bacterial reactions, which occurs more rapid in the presence of supplementary As(V), in comparison with that depicted in Ramirez-Aldaba
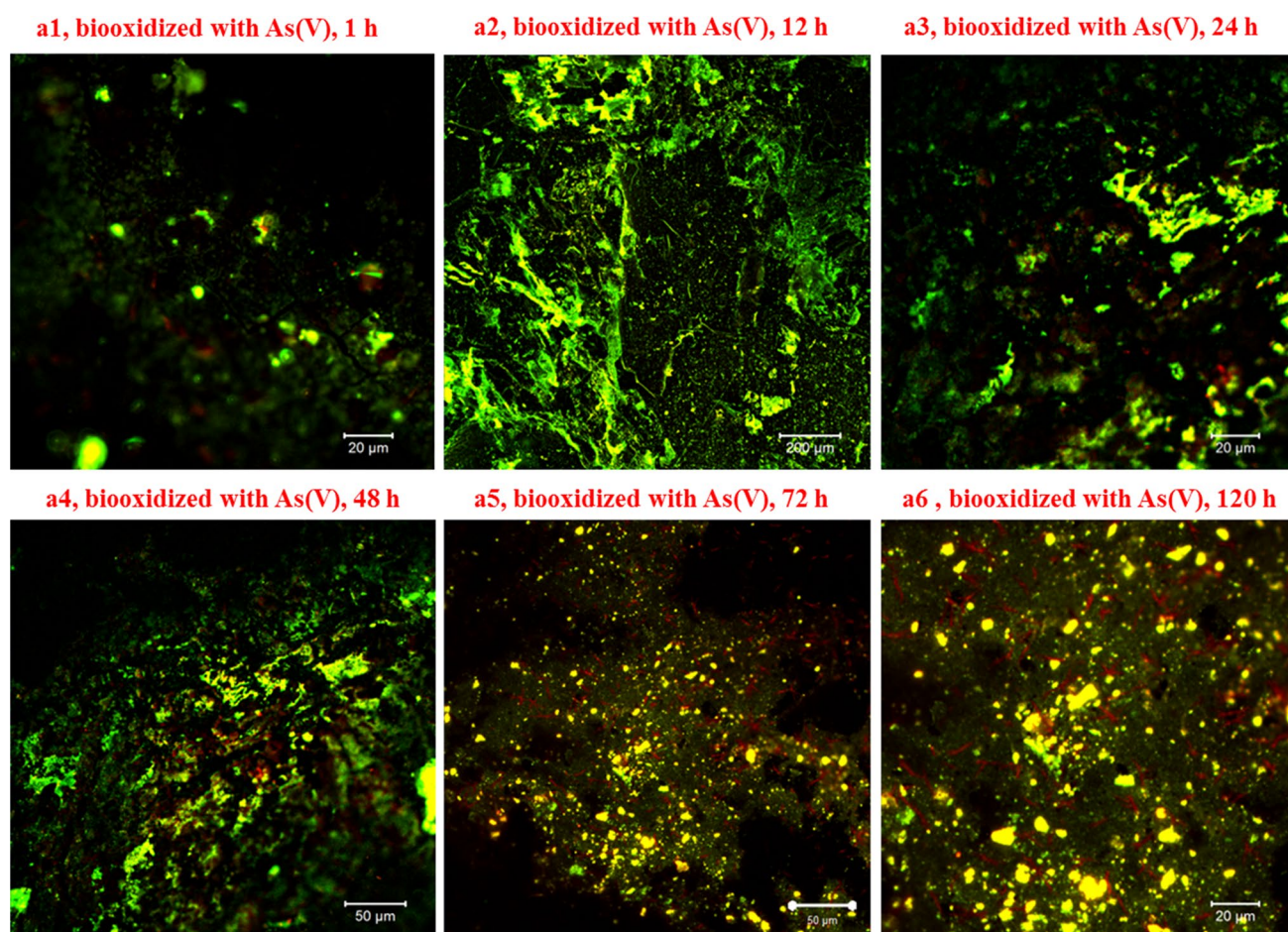
Fig. 5 CLSM images (merge) of *A. thiooxidans* for biofilms formed after the biooxidation of eMAE surfaces under the influence of supplementary As(V) after 1 h (**a1**), 12 h (**a2**), 24 h (**a3**), 48 h (**a4**), 72 h (**a5**) and 120 h (**a6**) of assay. Original epifluorescence of hydrophobic domains as exopolysaccharides is shown in green and the original contribution of hydrophobic domains is in red. Merge is appreciated as a transition from yellow to red. Scanning areas of 300×300 µm

et al. [12] (i.e. without As). Note that the increment of bacterial EPS is a typical response of microorganisms to face stressing environment and conditions (i.e. pH, As, heavy metals, temperature) [2, 39, 41], in agreement with Figs. 3, 4, 5; helping to determine structure and function of extracellular lipids in stressed biofilms (i.e. leaching cells).

The highest surface hydrophobicity was then identified after 120 h of assay in the presence of supplementary As(V) (Fig. 5a6). Altered arsenopyrite surface was mainly dominated by abundant hydrophobic secondary pyrite-like, S_n^{2-} and S^0 compounds (Figs. 1, 2, 3), as well as stressed biofilms with higher secretion of extracellular lipids (i.e. lipopolysaccharides) (Figs. 4, 5, S4, Table S4) [17]. The rapid establishment of hydrophobic biofilms after 12 h (Fig. 5a2, Table S4) relies on the configuration of a more stable biofilm and its progressive enclosure in secondary products (i.e. pyrite-like, S_n^{2-}, S^0) (Figs. S4b″, 4b5). According to literature, biofilm structures organize and evolve depending on substrate properties and their electrochemical

characteristics [40, 42, 43]. While bacterial reactions promote secretion of extracellular lipoproteins and fatty acids to sustain bioleaching activity [15, 44]; these characteristics (i.e. biofilm, surface-bulk structure) can be significantly modified by influence of toxic microenvironments (i.e. As (V)). Therefore, these data confirm a strong relationship between chemical surface speciation (i.e. 1–6 µm depth) and bacterial reactions to supplementary As(V).

Table 1 shows the quantification of extracellular surface proteins forming biofilms (i.e. EPS-associated protein fraction) for all times in the presence of supplementary As(V). Quantification of the corresponding extracellular surface proteins in the absence of supplementary As(V) is presented in Ramirez-Aldaba et al. [12], for comparison purposes. A general diminution of extracellular surface proteins was observed for all the experiments, which adequately agrees with observations for biofilm evolution (Figs. 4, 5, S4, Table 1). Not surprisingly, lower protein production was identified for stressed biofilms, regarding protein production

Table 1 Extracellular surface proteins of biofilms during biooxidation of eMAE surfaces with As(V) by *A. thiooxidans* at different times

Biooxidation time (hours)	Extracellular surface proteins under the presence of toxic As(V) μg cm^{-2} ± SD
1	1.2 ± 0.1
12	1.8 ± 0.1
24	2.6 ± 0.05
48	4.1 ± 0.08
72	4.8 ± 0.1
120	4.3 ± 0.1

Extracellular surface proteins on planktonic cells in the presence of supplementary As(V) are 1.7 mg L^{-1} as reference

SD standard deviation

without the effect of supplementary As(V) [12]. These proteins ranged from 1.2 to 4.3 μg cm^2, indicating a general decreasing range from 28 to 40% (i.e. damaged biofilm). The highest protein production was observed between 24 and 48 h, which corresponded to specific point where biofilm organization was changed from incipient structure to compact-flattened micro-colonies in the presence of supplementary As(V) (Figs. 4, 5, Table 1). This suggested an adaptation period of cells to As(V) during biooxidation (i.e. 1–12 h), followed by minor and sustained biooxidation capacity [14, 24, 25]. Additionally, Devasia and Natarajan [15] distinguished proteinaceous compounds on the surface of *A. ferrooxidans* cells attached to pyrite, whence they concluded that an induction of relatively hydrophobic proteins is required for cell attachment to S_n^{2-} and S^0 compounds [45], in agreement with our findings (Fig. 5, Tables S4 and 1). Hence, the reduction of extracellular surface proteins revealed stages of difference sensibility of *A. thiooxidans* biofilms responding to arsenopyrite interactions and supplementary As(V) adaptation. According with Figs. 1, 2, 3, 4, 5 (and Tables S4 and 1), after initial sluggishness (i.e. 1 h) bacterial activity was still active in the presence of supplementary As(V), as described by extracellular surface proteins behavior together with changes in chemical speciation (i.e. concentration vs. depth profiles). These facts agree with observations made for microorganisms previously adapted to As species (i.e. *A. ferrooxidans, Leptospirillum ferrooxidans, Acidithiobacillus caldus*) [23, 31, 41], whereby our results exhibit intermediate stages comprising biooxidation process in the presence of supplementary As(V). These results confirmed a change in a transient biooxidation mechanism, which relies on the status of the *A. thiooxidans* and arsenopyrite interactions (i.e. stressed biofilms) [46]. Further studies (i.e. proteomics and bioinformatics approach) will be devoted to analyze the influence of supplementary As(V) on bacterial responses facing challenging environments, thus, increasing the knowledge of protein production in the presence of As(V) for leaching bacteria. Indeed, this research could assist the identification of sensitive parameters accounting for changes in biofilm structure and performance during arsenopyrite biooxidation. The transient molecular response of the biofilms can be significantly elucidated by testing other relevant environmental conditions, such as heavy metals, various forms of arsenic and the inclusion of different mineral compounds in the system [37, 41]. Indeed, this analysis could reveal new insights regarding bacterial reactions (i.e. sensitive factors) during arsenopyrite biooxidation by *A. thiooxidans* and/or mixed cultures (i.e. *A. thiooxidans* and *A. ferrooxidans*) [18, 42].

Conclusions

The present study provides a new perspective disclosing crucial stages of *A. thiooxidans* and arsenopyrite interactions affected by supplementary As(V) after 5 days. Particular emphasis is placed to illustrate arsenopyrite surface-bulk changes (i.e. concentration depth-profiles) resulting from stressed biofilm performance. Raman, XPS, SEM–EDS, CLSM, GDS and EPS-associated protein fraction were synergistically combined to determine the following findings in the presence of supplementary As(V), regarding previous observations [11, 12]: (1) Surface hydropathy overcomes rapid change from hydrophilic (i.e. exopolysaccharides) to hydrophobic (i.e. extracellular lipids) character occurring at early biooxidation stages (i.e. 1–12 h). (2) Formation of more compact-flattened microcolonies with higher production of bacterial EPS after 24 h. (3) Progressive cells covered by abundant amount of secondary products after 120 h. (4) Sluggish initial biooxidation process (i.e. 1 h). (5) General diminution of extracellular surface proteins for stressed biofilms, in comparison with non-stressed biofilms. (6) Significant variations in arsenopyrite reactivity (i.e. concentration-depth profiles), and (7) Change in biooxidation mechanisms as a consequence of aforementioned bacterial reactions in the presence of supplementary As(V).

References

1. Bhattacharya P, Welch AH, Stollenwerk KG, McLaughlin MJ, Bundschuh J, Panaullah G (2007) Arsenic in the environment:

biology and chemistry. Sci Total Environ 379:109–120. https://doi.org/10.1016/j.scitotenv.2007.02.037

2. Kruger MC, Bertin PN, Heipieper HJ, Arsène-Ploetze F (2013) Bacterial metabolism of environmental arsenic-mechanisms and biotechnological applications. Appl Microbiol Biotechnol 97:3827–3841. https://doi.org/10.1007/s00253-013-4838-5

3. Wang S, Zhao X (2009) On the potential of biological treatment for arsenic contaminated soils and groundwater. J Environ Manag 90:2367–2376. https://doi.org/10.1016/j.jenvman.2009.02.001

4. Drewniak L, Sklodowska A (2013) Arsenic-transforming microbes and their role in biomining processes. Environ Sci Pollut Res 20:7728–7739. https://doi.org/10.1007/s11356-012-1449-0

5. Rohwerder T, Gehrke T, Kinzler K, Sand W (2003) Bioleaching review part A. Appl Microbiol Biotechnol 63:239–248. https://doi.org/10.1007/s00253-003-1448-7

6. Rohwerder T, Sand W (2007) Mechanisms and biochemical fundamentals of bacterial metal sulfide oxidation. In: Microbial processing of metal sulfides, pp 35–58. Springer, Berlin. https://doi.org/10.1007/1-4020-5589-7_2

7. Sasaki K, Tsunekawa M, Ohtsuka T, Konno H (1998) The role of sulfur-oxidizing bacteria *Thiobacillus thiooxidans* in pyrite weathering. Coll Surf A 133:269–278. https://doi.org/10.1016/S0927-7757(97)00200-8

8. Zhang J, Zhang X, Ni Y, Yang X, Li H (2007) Bioleaching of arsenic from medicinal realgar by pure and mixed cultures. Process Biochem 42:1265–1271. https://doi.org/10.1016/j.procbio.2007.05.021

9. Ko MS, Park HS, Kim KW, Lee JU (2013) The role of *Acidithiobacillus ferrooxidans* and *Acidithiobacillus thiooxidans* in arsenic bioleaching from soil. Environ Geochem Health 35:727–733. https://doi.org/10.1007/s10653-013-9530-2

10. Liu H, Gu G, Xu Y (2011) Surface properties of pyrite in the course of bioleaching by pure culture of *Acidithiobacillus ferrooxidans* and a mixed culture of *Acidithiobacillus ferrooxidans* and *Acidithiobacillus thiooxidans*. Hydrometallurgy 108:143–148. https://doi.org/10.1016/j.hydromet.2011.03.010

11. Ramírez-Aldaba H, Valles OP, Vazquez-Arenas J, Rojas-Contreras JA, Valdez-Perez D, Ruiz-Baca E, Meraz M, Lara RH (2016) Chemical and surface analysis during evolution of arsenopyrite oxidation by *Acidithiobacillus thiooxidans* in the presence and absence of supplementary arsenic. Sci Total Environ 566:1106–1119. https://doi.org/10.1016/j.scitotenv.2016.05.143

12. Ramírez-Aldaba H, Vazquez-Arenas J, Sosa-Rodríguez FS, Valdez-Pérez D, Ruiz-Baca E, García-Meza JV, Trejo-Córdoba G, Lara RH (2017) Assessment of biofilm changes and concentration-depth profiles during arsenopyrite oxidation by *Acidithiobacillus thiooxidans*. Environ Sci Pollut Res 24:20082–20092. https://doi.org/10.1007/s11356-017-9619-8

13. Mohammed-Abdul KS, Jayasinghe SS, Chandana EP, Jayasumana C, De Silva PMC (2015) Arsenic and human health effects: a review. Environ Toxicol 40:828–846. https://doi.org/10.1016/j.etap.2015.09.016

14. Rawlings DE (2008) High level arsenic resistance in bacteria present in biooxidation tanks used to treat gold-bearing arsenopyrite concentrates: a review. Trans Non Metals Soc China 18:1311–1318. https://doi.org/10.1016/S1003-6326(09)60003-0

15. Devasia P, Natarajan KA (2010) Adhesion of *Acidithiobacillus ferrooxidans* to mineral surfaces. Int J Miner Process 94:135–139. https://doi.org/10.1016/j.minpro.2010.02.003

16. Yu ZJ, Yu RL, Liu AJ, Jing L, Zeng WM, Liu XD, Qiu GZ (2017) Effect of pH values on extracellular protein and polysaccharide secretions of *Acidithiobacillus ferrooxidans* during chalcopyrite bioleaching. Trans Non Metals Soc China 27:406–412. https://doi.org/10.1016/S1003-6326(17)60046-3

17. Bobadilla-Fazzini RA, Levican G, Parada P (2011) *Acidithiobacillus thiooxidans* secretome containing a newly described

18. Deng S, Gu G, Wu Z, Xu X (2017) Bioleaching of arsenopyrite by mixed cultures of iron-oxidizing and sulfur-oxidizing microorganisms. Chemosphere 185:403–411. https://doi.org/10.1016/j.chemosphere.2017.07.037

19. Harneit K, Göksel A, Kock D, Klock JH, Gehrke T, Sand W (2006) Adhesion to metal sulfide surfaces by cells of *Acidithiobacillus ferrooxidans*, *Acidithiobacillus thiooxidans* and *Leptospirillum ferrooxidans*. Hydrometallurgy 83:245–254. https://doi.org/10.1016/j.hydromet.2006.03.044

20. Harneit K, Sand W (2007) Influence of growth substrate and attachment substratum on EPS and biofilms formation by *Acidithiobacillus ferrooxidans* A2. Adv Mat Res 20:385. https://doi.org/10.4028/www.scientific.net/AMR.20-21.385

21. Pinet N, Tremblay A (2009) Structural analysis of the Velardeña mining district, Mexico: a faulted Au-Ag-rich hydrothermal system. Can J Earth Sci 46:123–138. https://doi.org/10.1139/E09-007

22. Collinet MN, Morin D (1990) Characterization of arsenopyrite oxidizing *Thiobacillus*. Tolerance to arsenite, arsenate, ferrous and ferric iron. Antonie Van Leeuwenhoek 57:237–244. https://doi.org/10.1007/BF00400155

23. Leng F, Li K, Zhang X, Li Y, Zhu Y, Lu J, Li H (2009) Comparative study of inorganic arsenic resistance of several strains of *Acidithiobacillus thiooxidans* and *Acidithiobacillus ferrooxidans*. Hydrometallurgy 98:235–240. https://doi.org/10.1016/j.hydromet.2009.05.004

24. Dopson M, Baker-Austin C, Koppineedi PR, Bond PL (2003) Growth in sulfidic mineral environments: metal resistance mechanisms in acidophilic micro-organisms. Microbiology 149:1959–1970. https://doi.org/10.1099/mic.0.26296-0

25. Koechler S, Farasin J, Cleiss-Arnold J, Rsène-Ploetze F (2015) Toxic metal resistance in biofilms: diversity of microbial responses and their evolution. Res Microbiol 166:764–773. https://doi.org/10.1016/j.resmic.2015.03.008

26. Nöel N, Florian B, Sand W (2010) AFM and EFM study on attachment of acidophilic leaching organisms. Hydrometallurgy 104:370–375. https://doi.org/10.1016/j.hydromet.2010.02.021

27. Lu P, Zhu C (2011) Arsenic Eh–pH diagrams at 25 C and 1 bar. Environ Earth Sci 62:1673–1683. https://doi.org/10.1007/s12665-010-0652-x

28. Bradford L (1976) A rapid and sensitive method for the quantification of microgram quantities of protein utilizing the principle of protein dye binding. Anal Biochem 72:248–252. https://doi.org/10.1016/0003-2697(76)90527-3

29. Comte S, Guibaud G, Baudu M (2006) Relations between extraction protocols for activated sludge extracellular polymeric substances (EPS) and complexation properties. Part I. Comparison of the efficiency of eight EPS extraction methods. Enzyme Microb Technol 38:237–245. https://doi.org/10.1016/j.enzmictec.2005.06.010

30. Elzeky M, Attia YA (1995) Effect of bacterial adaptation on kinetics and mechanisms of bioleaching ferrous sulfides. Chem Eng J Biochem Eng J 56:B115–B124. https://doi.org/10.1016/0923-0467(94)06086-X

31. Park J, Han Y, Lee E, Choi U, Yoo K, Song Y, Kim H (2014) Bioleaching of highly concentrated arsenic mine tailings by *Acidithiobacillus ferrooxidans*. Sep Purif Technol 133:291–296. https://doi.org/10.1016/j.seppur.2014.06.054

32. Hu X, Cai Y, Zhang Y (2017) Hydrothermal alteration of arsenopyrite by acidic solutions. Appl Geochem 77:102–115. https://doi.org/10.1016/j.apgeochem.2016.08.009

33. Mycroft JR, Bancronft GM, McIntyre NS, Lorimer JW, Hill IR (1990) Detection of sulphur and polysulphides on electrochemically oxidized pyrite surfaces by X-ray photoelectron spectroscopy

and Raman spectroscopy. J Electroanal Chem Interf Electrochem 292:139–152. https://doi.org/10.1016/0022-0728(90)87332-E

34. Nesbitt HW, Muir IJ (1998) Oxidation states and speciation of secondary products on pyrite and arsenopyrite reacted with mine waste waters and air. Miner Petrol 62:123–144. https://doi.org/10.1007/BF01173766

35. Jones RA, Koval SF, Nesbitt HW (2003) Surface alteration of arsenopyrite (FeAsS) by *Thiobacillus ferrooxidans*. Geochim Cosmochim Acta 67:955–965. https://doi.org/10.1016/S0016-7037(02)00996-1

36. Li J, Lu J, Lu X, Tu B, Ouyang B, Han X, Wang R (2015) Sulfur transformation in microbially mediated pyrite oxidation by *Acidithiobacillus ferrooxidans*: insights from X-ray photoelectron spectroscopy-based quantitative depth profiling. Geomicrobiol J 33:118–134. https://doi.org/10.1080/01490451.2015.1041182

37. Dave SR, Gupta KH (2007) Interactions of *Acidithiobacillus ferrooxidans* with heavy metals, various forms of arsenic and pyrite. Adv Mater Res 20:423–426. https://doi.org/10.4028/www.scientific.net/AMR.20-21.423

38. Liu HL, Chen BY, Lan YW, Cheng YC (2003) SEM and AFM images of pyrite surfaces after bioleaching by the indigenous *Thiobacillus thiooxidans*. Appl Microbiol Biotechnol 62:414–420. https://doi.org/10.1007/s00253-003-1280-0

39. Dheer R, Patterson J, Dudash M, Stachler EN, Bibby KJ, Stolz DB, Stolz JF (2015) Arsenic induces structural and compositional colonic microbiome change and promotes host nitrogen and amino acid metabolism. Toxicol Appl Pharmacol 289:397–408. https://doi.org/10.1016/j.taap.2015.10.020

40. Donlan MR (2002) Biofilms: microbial life on surfaces. Emerg Infect Dis 8:881–890. https://doi.org/10.3201/eid0809.020063

41. Zhang X, Feng YL, Li HR (2016) Enhancement of bio-oxidation of refractory arsenopyritic gold ore by adding pyrolusite in bioleaching system. Trans Nonferrous Metals Soc China 26:2479–2484. https://doi.org/10.1016/S1003-6326(16)64339-X

42. Crundwell FK (2015) The semiconductor mechanism of dissolution and the pseudo-passivation of chalcopyrite. Can Metall Q 54:279–288. https://doi.org/10.1179/1879139515Y.0000000007

43. Echeverría-Vega A, Dermargasso C (2015) Copper resistance, motility and the mineral dissolution behavior were assessed as novel factors involved in bacterial adhesion in bioleaching. Hydrometallurgy 157:107–115. https://doi.org/10.1016/j.hydromet.2015.07.018

44. Lawrence JR, Swerhone GDW, Leppard GG, Araki T, Zhang X, West MM, Hitchcock AP (2003) Scanning transmission X-ray, laser scanning, and transmission electron microscopy mapping of the exopolymeric matrix of microbial biofilms. Appl Environ Microbiol 69:5543–5554. https://doi.org/10.1128/AEM.69.9.5543-5554.2003

45. Arredondo R, García A, Jerez CA (1994) Partial removal of lipopolysaccharide from *Thiobacillus ferrooxidans* affects its adhesion to solids. Appl Environ Microbiol 60:2846–2851. http://aem.asm.org/content/60/8/2846.short

46. Kumar RN, Nagendran R (2007) Influence of initial pH on bioleaching of heavy metals from contaminated soil employing indigenous *Acidithiobacillus thiooxidans*. Chemosphere 66:1775–1781. https://doi.org/10.1016/j.chemosphere.2006.07.091